Supplementary Information (SI) for Journal of Materials Chemistry B.
This journal is © The Royal Society of Chemistry 2026

SUPPORTING INFORMATION

Selective Turn-On Fluorescent Sensing of Endogenous Glutamate Using N-CQDs/Al Nanocomposites in Zebrafish CNS

*Diptiman De [a,ft], Debasmita Baidya [bt], Shrodha Mondal [a], Santosh K. Jana [c], Sabyasachi Chakraborty [d,e], Sukhendu Mandal [c], Subhra P.Hui [*b] and Prithidipa Sahoo [*a]*

[a]Department of Chemistry, Visva-Bharati University, Santiniketan-731235, India.

[b]S. N. Pradhan Centre for Neurosciences, University of Calcutta, Kolkata 700019, India

[c]Department of Microbiology, University of Calcutta, Kolkata-700019, India

[d]Department of Chemistry, School of Engineering and Sciences (SEAS), SRM University AP, Amaravati 522240, Andhra Pradesh, India

[e]Centre for Interdisciplinary Research, SRM University AP, Amaravati 522240, Andhra Pradesh, India

[f]Department of Chemistry, Gushkara Mahavidyalaya, Guskara- 713128, India.

[*a]Correspondence to: Dr. Prithidipa Sahoo (Email: prithidipa.sahoo@visva-bharati.ac.in)

[*b]Correspondence to: Dr. Subhra Prakash Hui (Email: sphsnp@caluniv.ac.in)

[t] Equal contribution to this paper

Number of Pages: 19

Number of Tables: 5

Number of Figure: 19

Table of Contents

1. Performance comparison of different methods of Glutamate detection.

Table S1. Performance comparison of different methods of Glutamate detection.

Methods	Material applied	Limit of Detection	Application	References
Fluorometric	CQD	0.17 µM	Applications in food safety and environmental monitoring	1
Fluorometric	Carbon Dots (CD)	0.085 µM	-	2
Electrochemical	peptide aptamer-based amperometric sensor	0.0001 µM	Mouse serum sample	3
Fluorometric	Polydopamine Dots-Based Fluorescent Nanoswitch Assay	0.12 µM	Human Serum and living cell	4
Electrochemical	Glassy Carbon Microelectrodes	0.01 µM	-	5
Electrochemical	nano-porous pseudo carbon paste electrode (Nano-PPCPE)	0.25 µM	-	6
Fluorometric and Colorimetric	Lanthanide Metal–Organic Framework	3.6 µM	Blood plasma	7
Electrochemical	A glassy carbon electrode modified with C-dots and silver nanoparticles	1.6 µM	-	8
Fluorometric	bio-compatible carbon dots	0.0013 µM	In the real food sample	9
Electrochemical	Electrochemical Biosensor	0.25 µM	-	10
Electrochemical	biosensor based on platinum nanoparticles, carbon quantum dots and poly-L-aspartic acid	0.3 µM	In the serum sample	11
Fluorometric	carbon dots	-	In the rat brain nerve terminals	12
Fluorometric and Colorimetric	Gadolinium (III) doped carbon dots	0.0012 µM	Glutamate and Dopamine in mouse serum, human urine sample, and cells	13
Fluorometric	graphene quantum dot	0.052 µM	-	14
fast-scan cyclic voltammetry (FSCV)	glutamate microbiosensor	-	Glutamate and Dopamine in the Rat Striatum	15
Fluorometric	***N-CQDs/Al composite***	***0.14 µM***	***In Vivo and In Vitro Glutamate detection in zebrafish optic tectum and retina***	***Present work***

2. **Purification of N-CQDs:** Purification of N-CQDs: After centrifugation, the solution was filtered through a 0.22 μm membrane to remove large particles and aggregates. It was then purified by dialysis using a 1000 Da MWCO membrane for 24 hours, with occasional solvent changes to remove small molecular impurities and unreacted precursors. The resulting solution was lyophilized to produce a pale-yellow solid powder. The product's purity was confirmed by IR, NMR, and UV–Vis spectroscopy. Notably, a solid product also formed after filtration and showed the same IR, NMR, and UV–Vis spectra to those of the dialysed sample, indicating that its chemical composition remained unchanged during dialysis and that it shared the same purity.
3. ***In Vitro* Mammalian Cell Line Culture:** HeLa cell lines were prepared from continuous culture in Dulbecco's Modified Eagle's Medium (DMEM, Sigma Chemical Co., St. Louis, MO) supplemented with 10% fetal bovine serum (Invitrogen), penicillin (100 μg/mL), and streptomycin (100 μg/mL). At first cells were breed in 75 cm^2 polystyrene, filter–capped animal tissue culture flask in an atmosphere of 5% CO_2 and 95% air at 37°C in CO_2 incubator. When cells were reached the logarithmic phase, the cells density were adjusted to 1.0×10^5 per well in culture media and then used to inoculate with 1000 μL (1.0×10^5 cells) of cell suspension in each glass bottom dish. After the cell adhesion observation, culture medium was removed and the cell layer was rinsed two to three times with phosphate buffered saline (PBS) (pH 7.0), and then used according to the experimental requirements.
   HeLa cells were maintained in continuous culture in Dulbecco's Modified Eagle's Medium (DMEM; Sigma Chemical Co., St. Louis, MO, USA) supplemented with 10% (v/v) fetal bovine serum (FBS; Invitrogen), penicillin (100 μg/mL), and streptomycin (100 μg/mL). Cells were cultured in 75 cm^2 filter-capped polystyrene tissue culture flasks under standard conditions (37 °C, 5% CO_2, and 95% relative humidity) in a CO_2 incubator. Upon reaching the logarithmic growth phase, cells were harvested and the cell density was adjusted to 1.0×10^5 cells/mL. Subsequently, 1.0 mL of the cell suspension (1.0×10^4 cells per dish) was seeded into glass-bottom culture dishes and allowed to adhere. After confirming cell attachment, the culture medium was removed and the cell monolayer was gently washed two to three times with phosphate-buffered saline (PBS, pH 7.0). The cells were then processed further according to the specific experimental requirements.
4. **Assessment of Cell Viability Using the MTT Method:** Cell viability was assessed using a colorimetric MTT assay following the standard protocol described by.[16] HeLa cells were seeded into 96-well polystyrene tissue culture plates at a density of 7.5×10^3cells per well in 100 μL of complete culture medium and incubated for 24 h at 37 °C in a humidified atmosphere containing 5% CO_2 to allow cell attachment. After incubation, cells were treated in triplicate with various concentrations (30–120 μg/mL) of N-CQDs alone or N-CQDs in combination with aluminium and glutamate, prepared in complete medium.
   Following the treatment period, 20 μL of MTT solution was added to each well and the

plates were further incubated for 3.5 h to allow the formation of insoluble purple formazan crystals. Subsequently, 150 µL of MTT solvent was added to each well to dissolve the formazan crystals, and absorbance was measured using a Synergy H1 microplate reader (Agilent BioTek) at 590 nm. Wells containing medium, test compounds, and MTT reagent without cells served as blanks, while control wells containing cells, medium, and MTT reagent without test compounds were used as untreated controls.

5. **Microscopy-Based Cellular Imaging:** HeLa cells were employed for fluorescence imaging assays following previously described protocols. [17,18] Cells were seeded onto sterile 35 mm glass-bottom culture dishes at a density of 1.0×10^5 cells per dish in 1.0 mL of Dulbecco's Modified Eagle's Medium (DMEM) and incubated for 10 h at 37 °C in a humidified atmosphere containing 5% CO_2 to allow cell attachment. Thereafter, the cells were gently washed once with phosphate-buffered saline (PBS) and incubated with N-CQDs (30 µg/mL) prepared in DMEM for 1 h under identical incubation conditions. Following incubation, cells were washed three times with PBS (pH 7.0) to remove excess N-CQDs and immediately examined using an Olympus IX73 fluorescence microscope. Fluorescence images were acquired using an FITC filter set with excitation at 400 nm and emission collected at 550 nm. Subsequently, the cells were further incubated with aluminium (30 µg/mL) for 20 min, followed by three washes with PBS (pH 7.0) to remove unbound aluminium ions. The cells were then treated with glutamate (40 µg/mL) for 20 min, and excess reagent was removed by washing three times with PBS (pH 7.0). Final fluorescence imaging was performed using an FITC filter set with excitation at 400 nm and emission collected at 550 nm. To enable reliable comparison of intracellular fluorescence intensity across all images, microscope parameters, including transmission density and scan speed, were maintained constant throughout image acquisition.

6. ***In vivo* analysis**

   a) **Zebrafish Maintenance:**

   Wild-type (Tübingen) zebrafish were used to test the efficacy of N-CQDs in *in vivo* system. The fish were obtained from the Zebrafish International Resource Centre (ZIRC) and then maintained at 28°C on a 14-hr light/10-hr dark cycle. Studies were conducted after getting approval of the Institutional Ethics Committee (IEC) of the University of Calcutta (CPCSEA/ORG/CH/Reg. NO. 925/298) and were carried out according to the recommendations mentioned in the CPCSEA (Committee for the Purpose of Control and Supervision of Experiments on Animals, Ministry of Environments and Forests Government of India).

   b) **Methodology:**

To check the competence of the N-CQDs/Al complex for the *in vivo* detection of glutamate, the following steps were followed:

1) The survivability of the fish in different doses of N-CQDs (150 µg/ml, 100 µg/ml, 90 µg/ml), Al^{3+} (2.5 µg/ml, 2 µg/ml,1 µg/ml) with fixed dose of N-CQDs (90 ug/ml), and Glutamate (90 µg/ml, 70 µg/ml, 40 µg/ml) with fixed dose of N-CQDs (90 ug/ml) + Al^{3+} (1 ug/ml), selected based on prior studies, the *in vitro* experiment results and via trial and error procedure, were checked to determine the appropriate dose to be administered without causing any lethality to the fish (Fig. S1). [19-22]

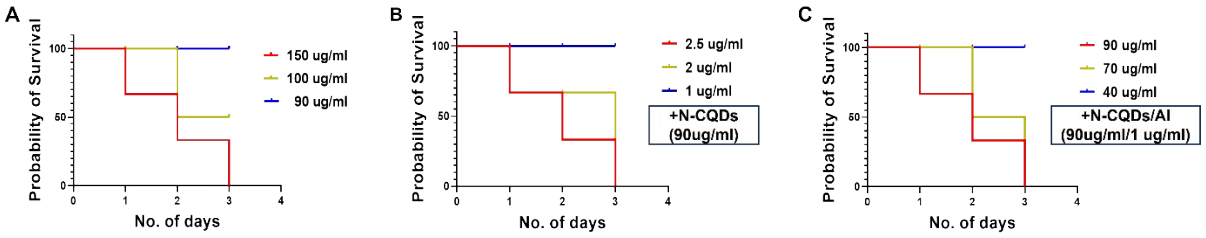

Fig. S1: Kaplan-Meier survival curves showing the survivability of zebrafish in different doses of A: N-CQDs; B: Al^{3+} with fixed dose of 90 ug/ml of N-CQDs for all the cases; C: Glutamate with fixed dose of 90 ug/ml of N-CQDs and 1 ug/ml of Al^{3+} for all the cases

2) The appropriate dose was selected to be 90 µg/ml for N-CQDs, 1 ug/ml for Al^{3+} along with fixed dose of N-CQDs (90 ug/ml) and 40 µg/ml for Glutamate along with fixed dose of N-CQDs (90 ug/ml) and Al^{3+} (1 ug/ml).
3) Three experimental conditions were set up:
   a. Fish were exposed to system tank water containing 90 ug/ml of N-CQDs for two days, overnight. Tissue was collected on the 3rd day.
   b. Fish were also exposed to system tank water containing N-CQDs/Al complex, with 1 ug/ml concentration and 90 µg/ml of N-CQDs of aluminium for two days, overnight. Tissue from ½ of the fish was collected on the 3rd day.
   c. The remaining ½ of the fish were exposed to system tank water containing N-CQDs/Al (90 µg/ml and 1 µg/ml, respectively) complex, along with glutamate (40 µg/ml), for the rescue experiment for two days, overnight. The tissue of these fish was collected on the 5th day.

Table S2. Details of the treatment procedure

Experimental condition	DAY 1	DAY 2	DAY 3	DAY 4	DAY 5
1.	N-CQDs	N-CQDs	Collection		
2.	N-CQDs/ Al	N-CQDs/ Al	Collection	Collection	
3.	N-CQDs/ Al	N-CQDs/ Al	N-CQDs/Al/ Glutamate	N-CQDs/ Al/ Glutamate	Collection

4) Cytotoxicity assessment in zebrafish:

Apart from checking for the survivability of the fish, uncoordinated movement, slow swimming, seclusion from the group or swimming towards the surface were observed to check for signs of stress and asphyxiation in fish. TUNEL assay was done on zebrafish liver cryosections to detect apoptotic cells for assessment of cytotoxicity. In Situ Cell Death Detection Kit, TMR red (Catalogue no. 12156792910) was used to perform the TUNEL assay. In comparison to the untreated controls, TUNEL-positive apoptotic cells were undetected in all three experimental conditions (Fig. S2).

5) Tissue collection, Sectioning and Microscopy

Zebrafish was anaesthetized using 0.02% Tricaine (MS222; Sigma, St. Louis, MO) in system water. Adult brain and retina were surgically collected and processed as per the standard procedure (Hui et al., 2017). The tissues were then fixed in 4% paraformaldehyde overnight, cryoprotected in 20% sucrose overnight (4°C) and embedded in Tissue freezing Medium. Tissues were sectioned into 20 µm slices by using a LEICA cryostat (CM3050). Tissue sections were dipped in PBT solution twice and then counterstained using Propidium iodide (1:100) and imaged using fluorescence microscope (Olympus BX53). For better contrast and representation, propidium iodide was portrayed as magenta color and DAPI as grey color in the image panel (Fig. 7, S2). The fluorescence microscopy images were processed with the help of ImageJ software (Fig. 9, S2).

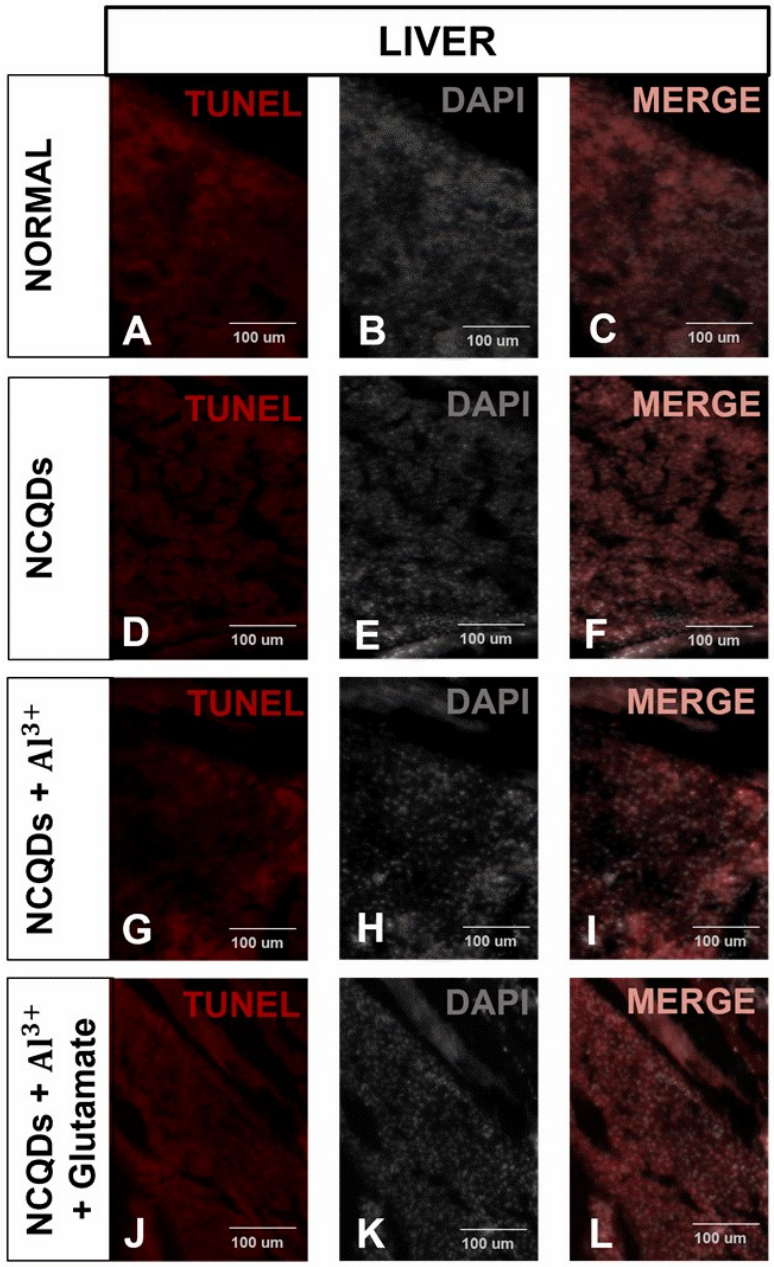

Fig. S2: TUNEL assay performed on zebrafish liver cryosections A-C: Untreated controls; D-F: N-CQDs-treated zebrafish liver section; G-I: N-CQDs/Al-treated zebrafish liver section; J-L: N-CQDs/Al/Glutamate-treated zebrafish liver section. The absence of TUNEL-positive apoptotic cells in all four conditions indicates the absence of cell death. Scale bar: 100 µm.

7. PXRD of N-CQDs

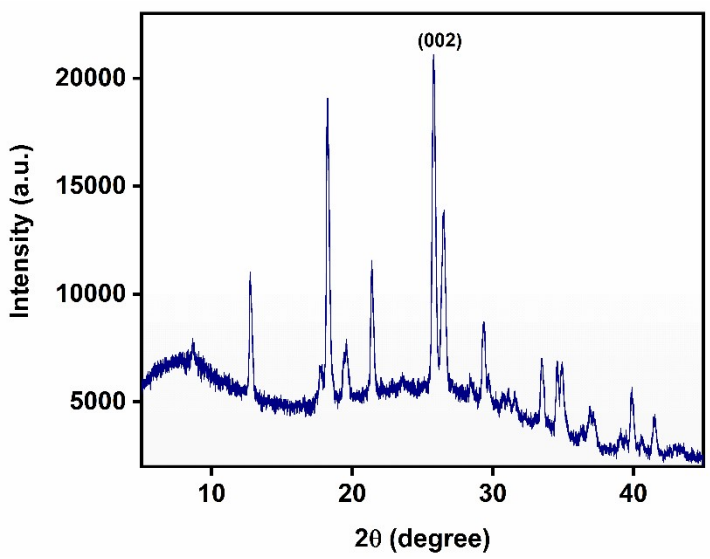

Fig. S3. PXRD of N-CQDs

8. Calculation of lattice spacing from SAED pattern

By calculating the distance between the rings in SAED, it is possible to determine the lattice spacing and identify Miller indices (Table S3). Also, JCDPS card No. 75-1621 shows that the lattice spacing of N-CQDs is well matched with the SAED pattern.[23]

Table S3. SAED pattern data

Sl. No.	1/2r (nm^{-1})	1/r (nm^{-1})	r (lattice spacing) nm	d-spacing (Å)	Miller indices (hkl)
1	5.778	2.889	0.34	3.4	(002)
2	9.142	4.571	0.21	2.1	(100)

9. EDX spectra of N-CQDs

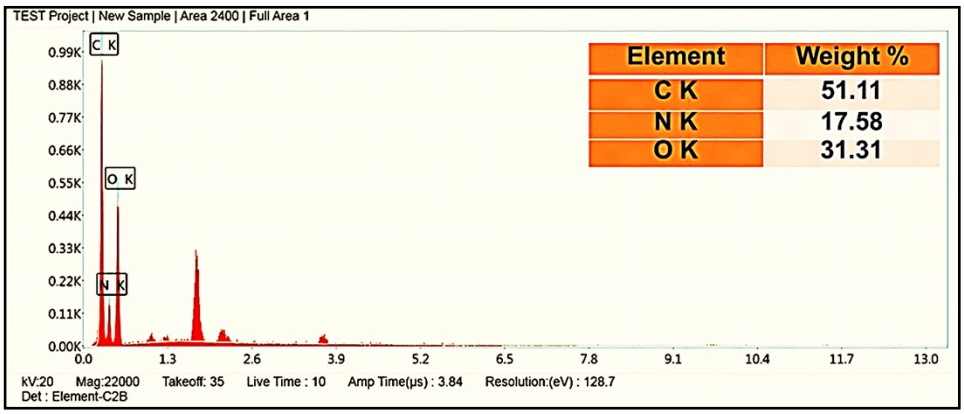

Fig. S4. EDX spectrum of N-CQDs (Atomic% of C k = 56.99, N k =16.81, O k = 26)

10. [1]HNMR of N-CQDs

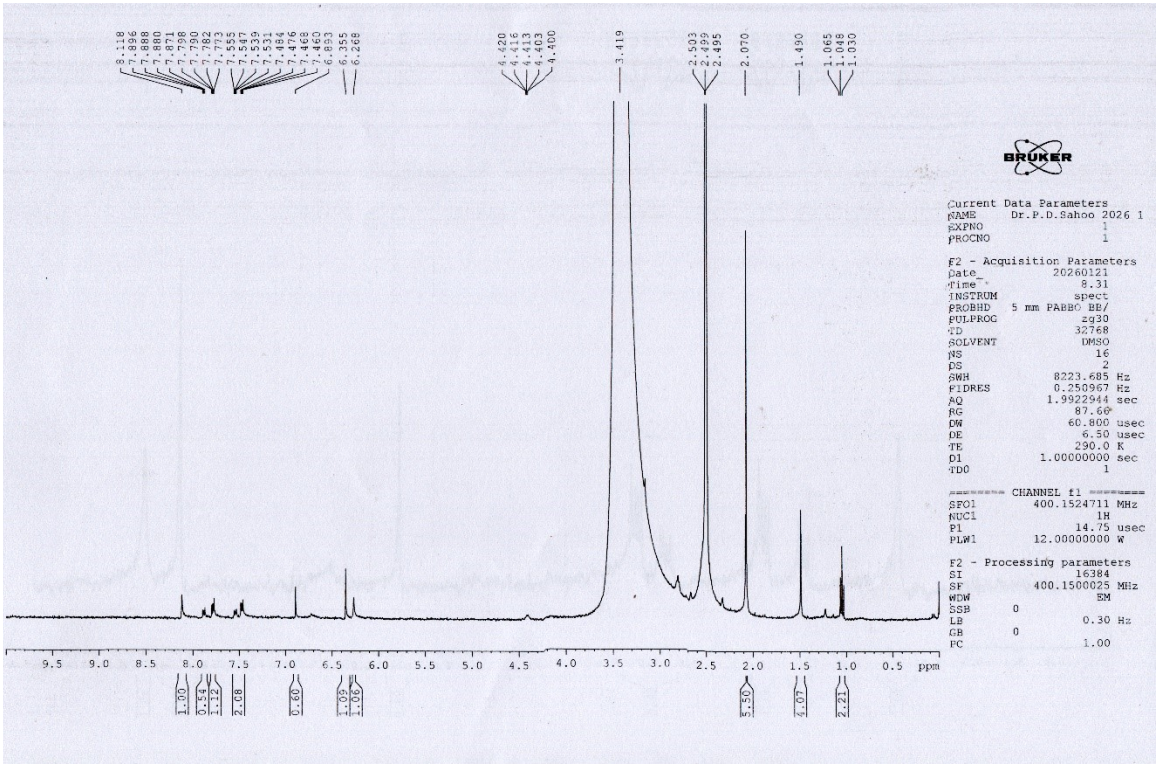

Fig. S5. [1]HNMR of N-CQDs in DMSO-d_6.

11. EDX spectra of N-CQDs/Al composite

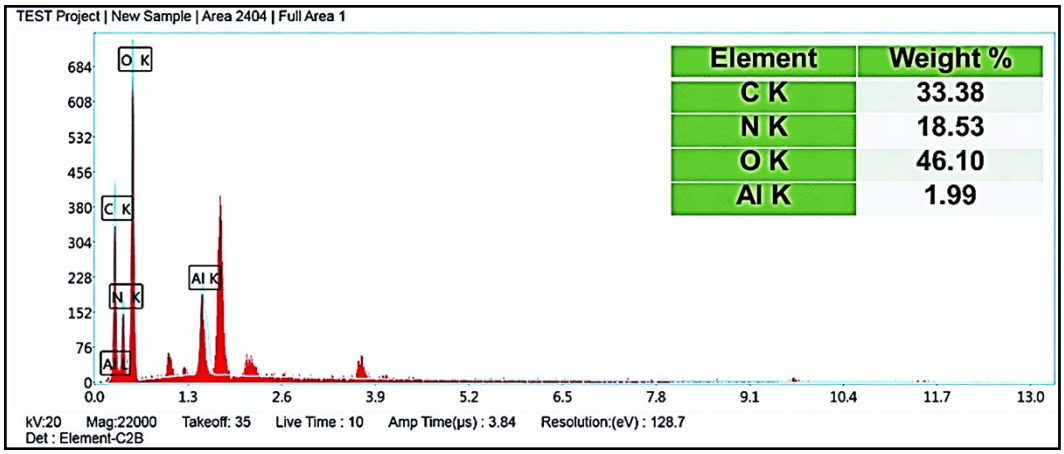

Fig. S6. EDX spectrum of N-CQDs/Al composite (Atomic % of C k = 39.39, N k= 18.74, O k = 40.83, Al k=1.05)

12. pH titration study

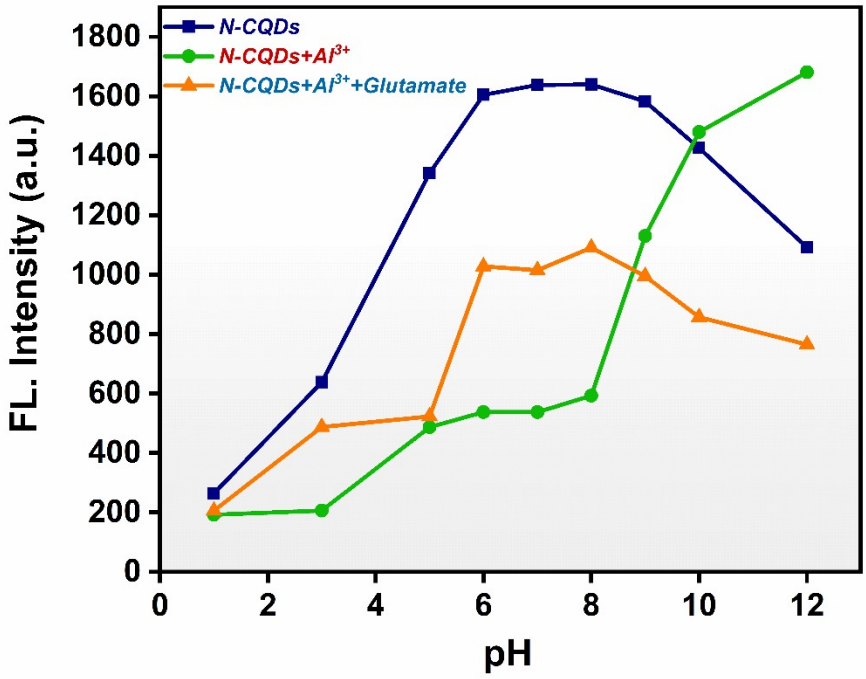

Fig. S7. pH response study of the N-CQDs, N-CQDs + Al^{3+} and N-CQDs + Al^{3+}+ Glutamate.

13. Photostability of N-CQDs

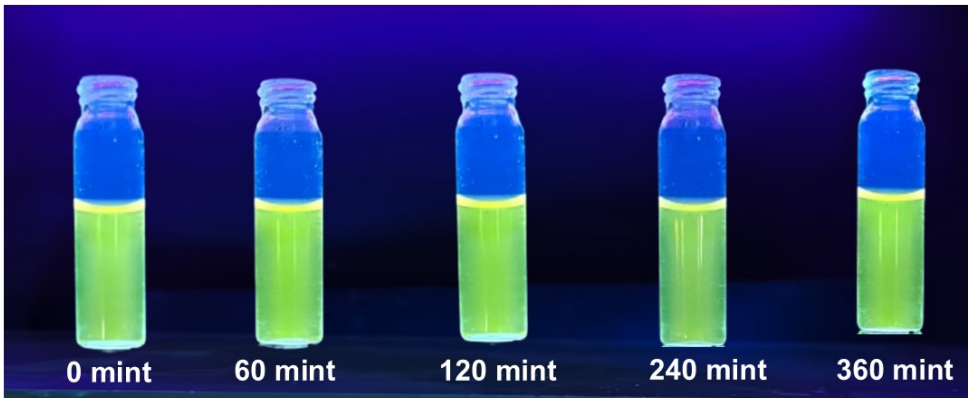

Fig. S8. Photostability test of N-CQDs under continuous irradiation of 365 nm UV light.

14. Selectivity

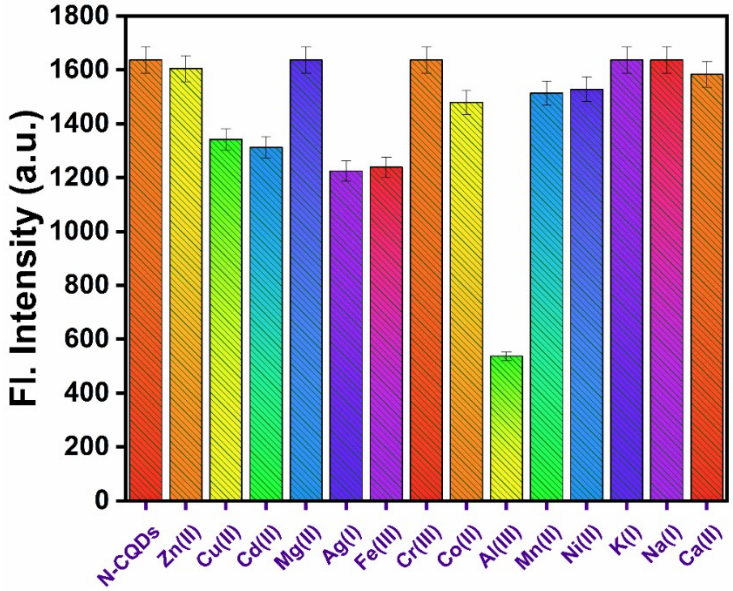

Fig. S9. Fluorescence spectra of N-CQDs in the presence of different metal ions at 548 nm (λ_{ex}= 400 nm).

15. Binding constant calculation graph (Fluorescence method)

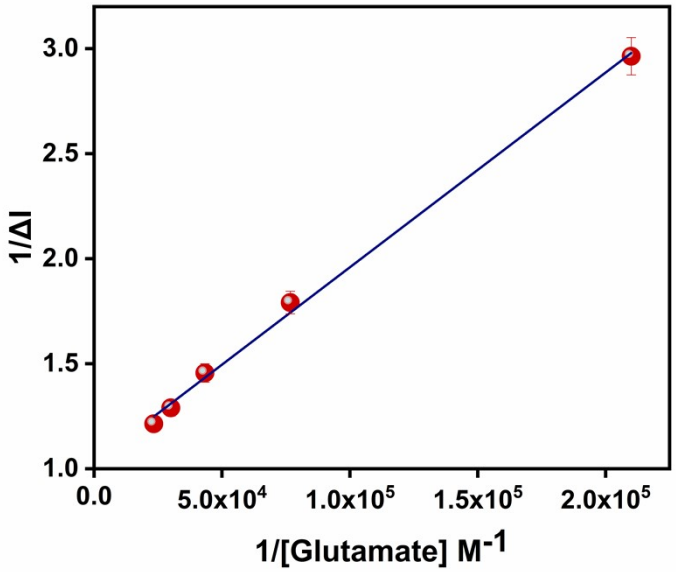

Fig. S10. Linear regression analysis for calculating the association constant value using the fluorescence titration method.

The association constant (K_a) of the N-CQDs/Al complex for glutamate sensing was determined from the equation K_a = intercept/slope. From the linear fit, we obtain an intercept of 1.03±0.03, a slope of (9.3±0.3)×10^{-6}, and a correlation coefficient (R^2) of 0.998. Thus, we get $\mathbf{K_a}$= (1.03)/ (9.3×10^{-6}) =**1.1×10^5 M^{-1}**

The standard free energy of binding is determined at 25 °C (298 K) using this equation

$$\Delta G^\circ = -RT\ln k$$

Using R=8.314 J $mol^{-1}K^{-1}$and T=298 gives

$$\Delta G^\circ \approx -28.7 \text{ kJ mol}^{-1}$$

16. Linear fit curve of N-CQDs/Al complex with Glutamate

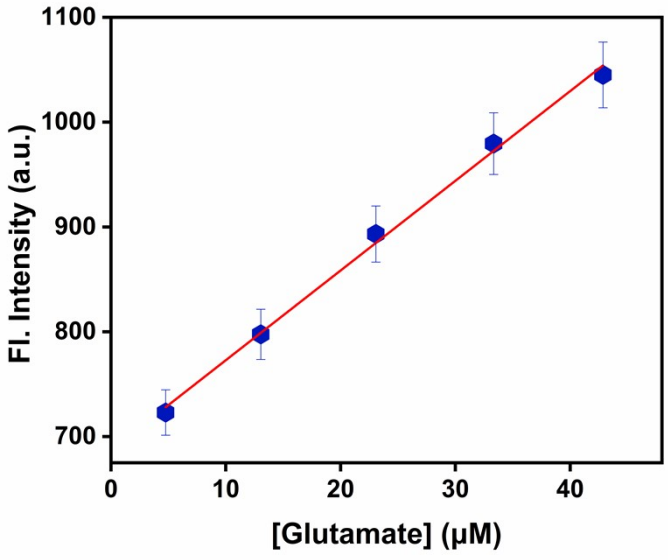

Fig. S11. Linear fit curve of **N-CQDs/Al** complex at 548 nm concerning **glutamate** concentration.

17. Calculation of Limit of Detection (LOD) and Limit of Quantification (LOQ) for Glutamate

Table S4. Calculation of Limit of Detection (LOD) and Limit of Quantification for Glutamate

Blank Reading (N-CQDs/Ag complex)	**Fluorescence Intensities at 486 nm (X)**	**Mean (X)**	**Standard Deviation (σ) = $\sqrt{\frac{\sum\|X-x\|^2}{N}}$**
Reading 1	537.6	537.4	0.405
Reading 2	538.0		
Reading 3	537.0		
Reading 4	536.9		
Reading 5	537.5		

Slope, m for glutamate = $(8.56\pm0.29)\times10^6$, intercept=687 ± 8, correlation coefficient (R^2) = 0.997

LOD for glutamate =$3\sigma/m = (3\times0.405)/ (8.56\times10^6) = 0.14\times10^{-6}$M= 0.14 μM

Determination of the limit of quantification (LOQ)

The limit of quantification (LOQ) = $10\sigma/m = (10\times0.405)/ (8.56\times10^6)$ = 0.47 μM

18. Competitive selectivity in the presence of other analytes

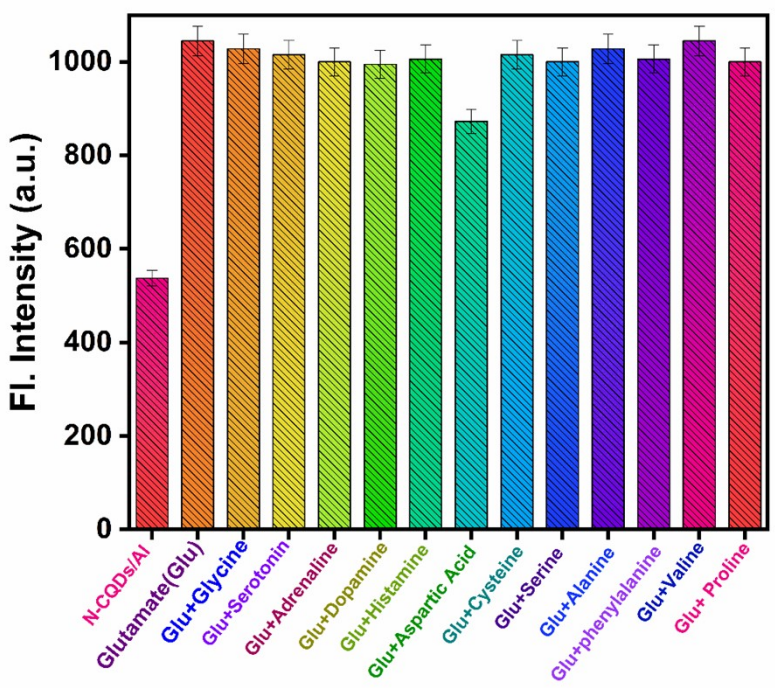

Fig. S12. Fluorescence spectra of N-CQDs/Al complex in the presence of different analytes (10^{-4} M) at 548 nm (λ_{ex}= 400 nm).

19. Fluorescence Titration of N-CQDs with Al^3

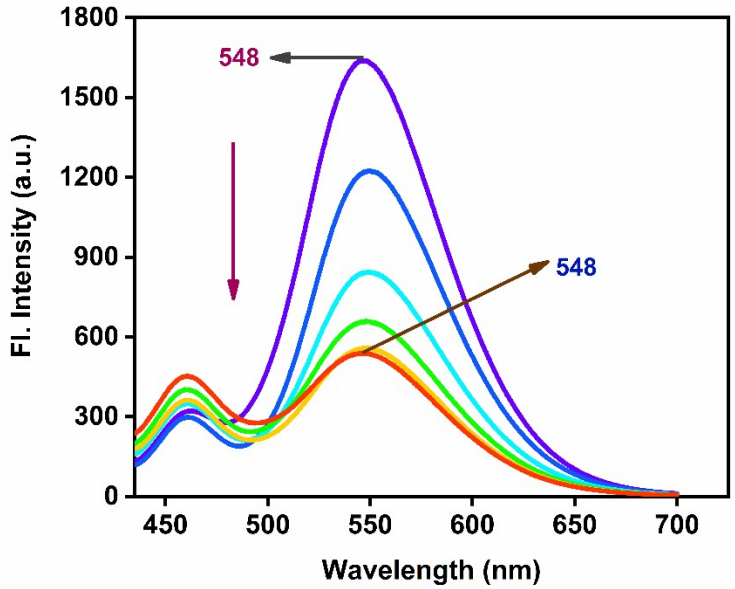

Fig. S13 At first, the N-CQDs solution was prepared by mixing 100 µL of stock N-CQDs solution (2 mg/mL) with 1.9 mL of buffer solution in a quartz cuvette, then the fluorescence of N-CQDs (pale violet) was quenched by the addition of different concentrations of Al^{3+} (10^{-3} M) (100 µM (blue), 170 µM (cyan blue), 230 µM (green), 285 µM (yellow), 330 µM (red)) at 400nm excitation.

20. UV-vis titration of N-CQDs with Al^{3+}

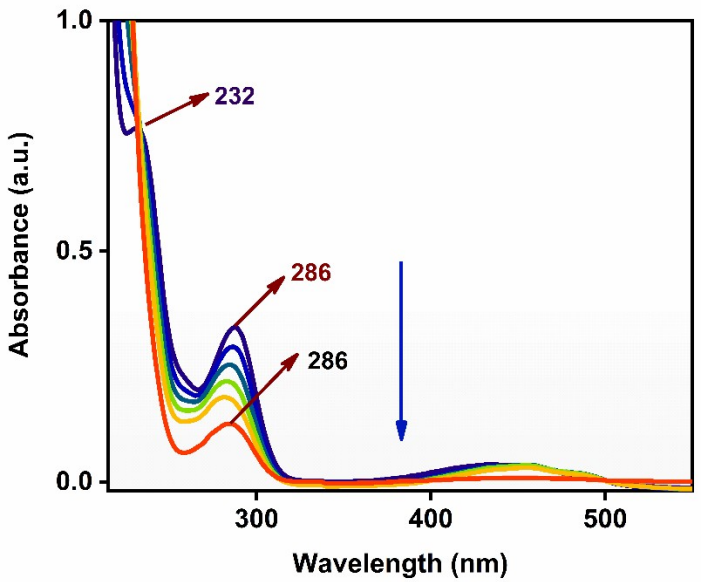

Fig. S14. UV-vis absorption spectra of N-CQDs upon addition of Al^{3+} (10^{-3} M).

21. Decay time components of N-CQDs, N-CQDs + Al^{3+} and N-CQDs + Al^{3+} + Glutamate

Table S5. Decay time components of N-CQDs, N-CQDs + Al^{3+} and N-CQDs + Al^{3+} + Glutamate

System	b_1	τ_1	b_2	τ_2	τ_3	b_3	$<\tau>=b_1\tau_1+b_2\tau_2+b_3\tau_3$
N-CQDs	0.54	0.0706806	0.36	1.55718	0.10	2.64899	**0.859 ns**
N-CQDs + Al^{3+}	0.09	0.96005	0.44	1.61934	0.46	0.0999362	**0.855 ns**
N-CQDs + Al^{3+} + Glutamate	0.35	1.35491	0.25	1.77519	0.40	0.100777	**0.956 ns**

22. HRTEM images of N-CQDs/Al and N-CQDs/Al + Glutamate:

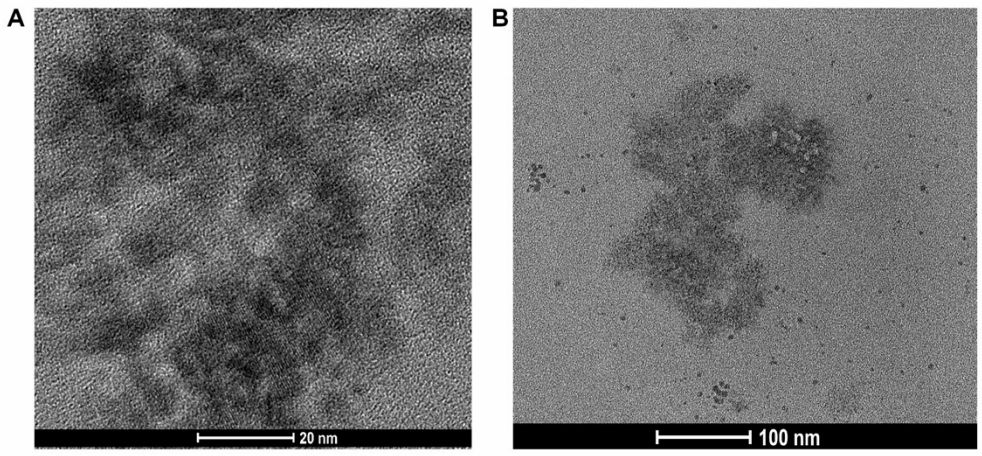

Fig. S15. H R TEM images of A) N-CQDs/Al and B) N-CQDs/Al + Glutamate

23. Fluorescence emission spectra

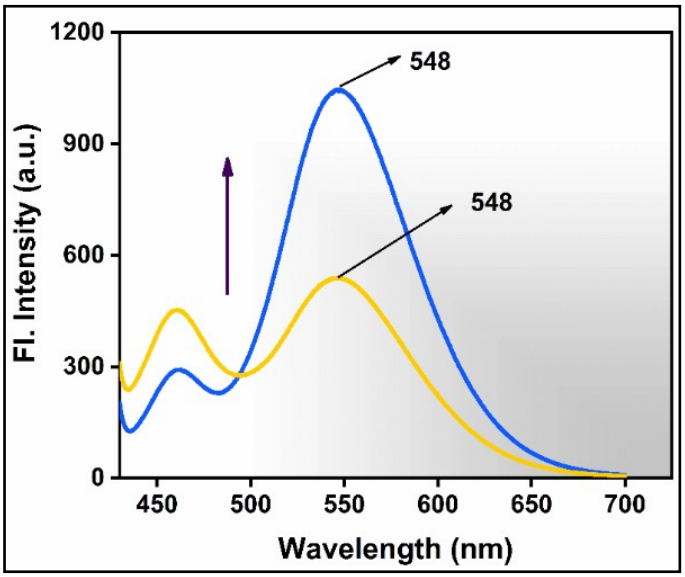

Fig. S16. Fluorescence emission spectra of N-CQDs/Al complex in the (1) absence (548 nm) and (2) presence of Glutamate (548 nm).

24. UV-vis titration of N-CQDs/Al complex with Glutamate

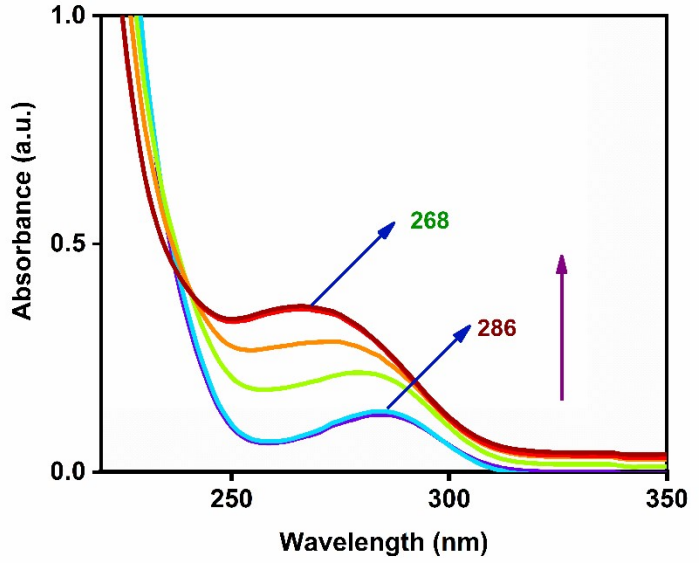

Fig. S17. UV-vis absorption spectra of N-CQDs/Al complex upon addition of Glutamate (10^{-4} M).

25. On-Off-On Fluorescence picture

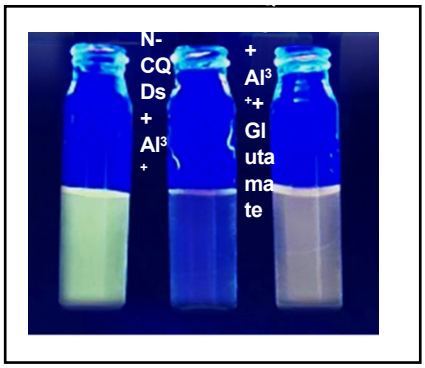

Fig. S18. On-Off-On Fluorescence image under a 365 nm UV lamp.

26. MTT Assay

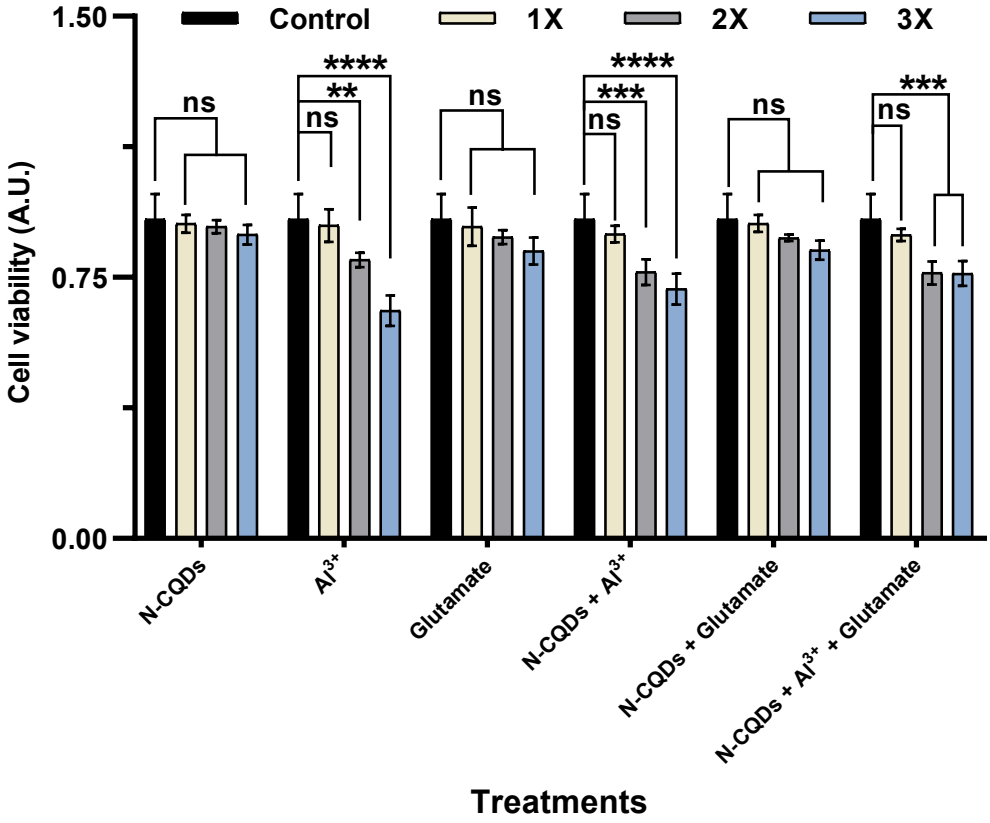

Fig. S19. MTT assay showing cytotoxicity of N-CQDs and their combinations in HeLa cells. Cells were treated with N-CQDs (1-3X:30, 60 & 90 µg/mL), Al^{3+} (1-3X: 30, 60 & 90 µg/mL), Glutamate (1-3X: 40, 80 & 120 µg/mL), and their binary and ternary combinations at 1X–3X doses (as indicated). Data are expressed as mean ± SE (n=3). Statistical analysis was performed using two-way ANOVA followed by Dunnett's multiple comparisons test (GraphPad Prism 8.0.1). Significance levels: "****" = $p<0.0001$, "***" =$p<0.001$, "**" =$p<0.01$, and "ns" = data is not significant.

Reference

1. Y. Ju and M. Zheng, *Anal. Chim. Acta*, **2025**, *1379*, 344742.
2. L. Yuan, L. Liu, Y. Bai, J. Qin, M. Chen and F. Feng, *Talanta*, **2022**, *245*, 123416.
3. W. Wang, Y. He, Y. Gao, H. Gao, L. Deng, Q. Gui, Z. Cao, Y. Yin and Z. Feng, *Bioelectrochemistry*, **2022**, *146*, 108165.
4. Q. Ci, J. Liu, X. Qin, L. Han, H. Li, H. Yu, K.-L. Lim, C.-W. Zhang, L. Li and W. Huang, *ACS Appl. Mater. Interfaces*, **2018**, *10*, 35760–35769.
5. S. L. Galindo, S. Nimbalkar, A. Oyawale, J. Bunnell, O. N. Cuacuas, R. Montgomery-Walsh, A. Rohatgi, B. K. Cariappa, A. Gautam and K. Peguero-Garcia *et al.*, *C*, **2024**, *10*, 68.
6. Y. Deng, W. Wang, L. Zhang, Z. Lu, S. Li and L. Xu, *J. Biomed. Nanotechnol.*, **2013**, *9*, 318–321.
7. T. Xia, Y. Wan, Y. Li and J. Zhang, *Inorg. Chem.*, **2020**, *59*, 8809–8817.
8. S. Zhu, X. Lin, P. Ran, F. Mo, Q. Xia and Y. Fu, *Microchim. Acta*, **2017**, *184*, 4679–4684.
9. M. Kumari, K. Banger, G. R. Chaudhary, S. Chaudhary, A. Umar, S. Akbar and S. Baskoutas, *J. Mol. Liq.*, **2023**, *388*, 122825.
10. Y. Deng, W. Wang, C. Ma and Z. Li, *J. Biomed. Nanotechnol.*, **2013**, *9*, 1378–1382.
11. C. K. Selvi, B. Şenceol and P. E. Erden, *Prep. Biochem. Biotechnol.*, **2025**, *55*, 309–317.
12. T. Borisova, A. Nazarova, M. Dekaliuk, N. Krisanova, N. Pozdnyakova, A. Borysov, R. Sivko and A. P. Demchenko, *Int. J. Biochem. Cell Biol.*, **2015**, *59*, 203–215.
13. S. Wei, B. Liu, X. Shi, S. Cui, H. Zhang, P. Lu, H. Guo, B. Wang, G. Sun and C. Jiang, *Talanta*, **2023**, *252*, 123865.
14. M. Hosseini, H. Khabbaz, A. S. Dezfoli, M. R. Ganjali and M. Dadmehr, *Spectrochim. Acta, Part A*, **2015**, *136*, 1962–1966.
15. L. C. Kimble, J. S. Twiddy, J. M. Berger, A. G. Forderhase, G. S. McCarty, J. Meitzen and L. A. Sombers, *ACS Sens.*, **2023**, *8*, 4091–4100.

16. T. Mosmann, *J. Immunol. Methods*, **1983**, *65*, 55–63.

17. J. Raut, R. D. Sherpa, S. K. Jana, S. M. Mandal, S. Mandal, S. P. Hui and P. Sahoo, *ACS Appl. Nano Mater.*, **2023**, *6*, 23611–23619.

18. D. De, S. K. Jana, S. Mondal, S. Mandal and P. Sahoo, *ACS Appl. Nano Mater.*, **2025**, *8*, 22038–22048.

19. S. Kaur, N. R. Selden and A. Aballay, *Front. Immunol.*, **2023**, *14*, 1093574.

20. M. L. Martins, E. F. Pinheiro, G. A. Saito, C. A. C. D. Lima, L. K. R. Leão, E. D. J. O. Batista, A. D. C. F. Passos, A. Gouveia, K. R. H. M. Oliveira and A. M. Herculano, *Front. Behav. Neurosci.*, **2024**, *18*, 1464992.

21. U. Roy, L. Conklin, J. Schiller, J. Matysik, J. P. Berry and A. Alia, *Sci. Rep.*, **2017**, *7*, 17305.

22. M. R. Senger, K. J. Seibt, G. C. Ghisleni, R. D. Dias, M. R. Bogo and C. D. Bonan, *Cell Biol. Toxicol.*, **2011**, *27*, 199–205.

23. A. Hemmati, H. Emadi and S. R. Nabavi, *ACS Omega*, **2023**, *8*, 20987–20999.